Journal Homepage: -www.journalijar.com

INTERNATIONAL JOURNAL OF ADVANCED RESEARCH (IJAR)

Article DOI:10.21474/IJAR01/24495
DOI URL: http://dx.doi.org/10.21474/IJAR01/24495

RESEARCH ARTICLE

PHYTOCHEMICAL CHARACTERIZATION AND IN-VITRO EVALUATION OF ANTISICKLING, ANTICOAGULANT, AND ANTI-INFLAMMATORY ACTIVITIES OF BARK EXTRACTS FROM ENANTIA CHLORANTHA AND ALSTONIA BOONEI

Elvis Jolinom Mbot, Noé Essono Kollo, Rony Mba Akue, Cédric Sima Obiang and Louis-Clément Obame Engonga

Manuscript Info

Manuscript History
Received: 18 August 2026
Final Accepted: 20 September 2026
Published: October 2026

Key words:-
Enantia chlorantha**,** Alstonia boonei**,** sickle cell disease, phytochemicals, traditional medicine, Gabon

Abstract

Background: Sickle cell disease (SCD) is a major hereditary hemoglo binopathy in sub - Saharan Africa. In Gabon, *Enantia chlorantha* and *Alstonia boonei* are widely used in ethnomedicine for managing sickle cell crises.

Objective: To conduct phytochemical analysis and evaluate antioxidan t, anti - inflammatory, antisickling, and anticoagulant activities of aqueous bark extracts of *E. chlorantha* and *A. boonei* in the context of traditional treatment of SCD.

Methods: Phytochemical screening and quantification of phenolic compounds were performed using standardized protocols. Antioxidant activity was assessed by DPPH radical scavenging and phosphomolybd enum assays. Anti-inflammatory potential was evaluated through protein denaturation and red blood cell hemolysis inhibition assays. Antisickling and anticoagulant activities were determined using the Emmel and Lee & White methods.

Results: Spectrophotometric quantification revealed marked differences in secondary metabolism: *A. boonei* exhibited higher baseline phenolic and proanthocyanidin levels, whereas E. chlorantha showed very high flavonoid enrichment (341.10 ± 6.77 mg QE/g). Both extracts exerted strong, dose - dependent anti - inflammatory effects, stabilizing erythrocyte membranes (IC_{50} = 65.40 µg/mL for E. chlorantha and 77.30 µg/mL for A. boonei) and effectively inhibiting protein denaturation (IC_{50} = 454.10 µg/mL and 419.50 µg/mL**,** respectively, comparable to diclofenac sodium**)**.Anticoagulant activity was notable, with E. chlorantha extending clotting time to 45.32 ± 2.59 min. Under sodium metabisulfite-induced hypoxia, both extracts achieved ~75% morphological reversion of sickled cells after 2 h, surpassing hydroxyurea ex vivo.

"© 2026 by the Author(s). Published by IJAR under CC BY 4.0. Unrestricted use allowed with credit to the author."

Conclusion: Aqueous bark extracts of Enantia chlorantha and Alstonia boonei show strong anti-inflammatory, antisickling, and anticoagulant activities, supporting ethnopharmacological use in Gabon; further studies should isolate active compounds.

Corresponding Author:- Elvis Jolinom Mbot

Introduction:-

Globally, an estimated 7.74 million individuals are affected by sickle cell disease (SCD), with approximately 515,000 children born with the condition each year, 79% of whom are in Sub-Saharan Africa [1,2]. Equatorial Guinea, Benin, Burkina Faso, Nigeria, Sierra Leone, and Togo together account for 44% of the global incidence at birth. In Gabon, one in four individuals carries the sickle cell trait (AS), regardless of ethnicity, geographic origin, or social class. Approximately 30,954 individuals are currently estimated to live with SCD in Gabon, for a projected national population of 2.31 million in 2025 [3,4].

Sickle cell disease remains a major public health concern, underscoring the urgent need for accessible therapeutic strategies. The pathophysiology of the disease is driven by HbS polymerization under hypoxic conditions [5,6]. Recent global advances include hydroxyurea (HU), blood transfusion, hematopoietic stem cell transplantation (HSCT), and emerging gene therapies [7,8]. However, in Africa, limited access to modern healthcare, shortage of medical personnel, and cultural practices mean that over 80% of the population relies on traditional medicine for self-care [9]. Numerous studies have demonstrated the antisickling activity of various plant extracts and natural dietary compounds, attributed mainly to anthocyanins**,** organic acids, and their derivatives [10],[11]. Among these, ***E. chlorantha*** and ***A. boonei*** are two medicinal plants widely used in Gabonese traditional medicine for managing sickle cell crises.

E. chlorantha (Annonaceae), known locally as **mfôl** (Fang), **ogowa** (Mpongwè, Galoa, Nkomi, Orungu), and **muguya** or **mwamba-lôlu** (Éshira), is a small tree with notable therapeutic properties. The roots and leaves of ***E. chlorantha*** have been reported to possess antisickling activity**,** attributed to Coenzyme Q10 [12,13]. The bark has been extensively studied for its antimalarial, antimicrobial, antibacterial, antioxidant, anticonvulsant, anti-inflammatory, analgesic, antiviral, gastroprotective**,** and fertility-enhancing activities [14],[15]. Its bioactive constituents, including alkaloids, flavonoids, phenols, saponins, reducing sugars, and cardiac glycosides, support its diverse pharmacological uses. Toxicological evaluations indicate that the extract is safe up to 500 mg/kg body weight [16].

A. boonei (Apocynaceae), known in Gabon as **ékuc** (Fang) or **mukuka** (Éshira, Bavili, Bapunu, Banzabi, Masangu), is a large forest tree with a cylindrical trunk. The stem bark has been reported to possess antisickling activity, primarily due to echitamines, alstonines, and reserpines [17],[18]. Pharmacological studies have also demonstrated antiplasmodial, antipyretic, anti-inflammatory, hepatoprotective, analgesic, antidiabetic, and trypanocidal activities, among others [19],[20]. The plant is rich in flavonoids, alkaloids, tannins, saponins, terpenes**,** and cardiac glycosides**,** which contribute to its multiple therapeutic applications. However, toxicity studies have shown hepato- and nephrotoxicity at doses ≥400 mg/kg**,** indicating the need for cautious use[21],[22]. Therefore, this study aimed to characterize phytochemicals and evaluate the pharmacological activities of aqueous bark extracts of *E. chlorantha* and *A. boonei* in the management of SCD.

Material and Methods:-

Biological Materials:-

Blood:-

Blood samples used for the anti-sickling evaluation were obtained from **two** (N = 2) healthy volunteer participants carrying the heterozygous sickle cell trait (HbAS genotype). Eligibility criteria required confirmation of the HbAS status by hemoglobin electrophoresis and the absence of blood transfusion within the four months preceding sample collection. Although individuals with the HbAS genotype are clinically asymptomatic, their erythrocytes were subjected to acute chemical hypoxia to induce structural sickling **in vitro**, thereby serving as an experimental model for sickle cell distortion. All volunteers were recruited on site at the Biochemistry Research Laboratory, where venous blood was collected into EDTA tubes. The study was conducted in accordance with the principles of the Declaration of Helsinki, and written informed consent was obtained from all participants prior to enrollment. The study protocol was reviewed and approved by the Gabon National Ethics Committee (approval number: 006/ December 2024). All samples were used strictly in compliance with the approved ethical guidelines.

Plant Material:-

The barks of **E. chlorantha** Oliv (Annonaceae) and **A. boonei** Wild (Apocynaceae) were collected respectively in June 2021 from the 3rd district of Libreville for **E. chlorantha**, and in June 2019 from Maboukou quarter, located in the 3rd district of Franceville for **A. boonei** (Gabon). The botanical identification of *E. chlorantha* and *A. boonei* was confirmed using the taxonomic database Plants of the World Online (POWO), maintained by Kew Gardens.

Taxonomic confirmation: *E. chlorantha* Oliv. [POWO ID: urn:lsid:ipni.org: names:771041-1] and *A. boonei* Wild. [POWO ID: urn:lsid:ipni.org:names:76511-1]. The botanical identification of the specimens was performed at the Institut de Pharmacopée et de Médecine Traditionnelle (IPHAMETRA), where voucher specimens were deposited under the reference numbers Bourobou 591 for **E. chlorantha** and JM Moussavou 1410 for **A. boonei**. Another portion of each sample was transferred to the Laboratoire de Recherche en Biochimie (LAREBIO)**,** Department of Chemistry, Faculty of Science**,** Université des Sciences et Techniques de Masuku (USTM)**,** Franceville, Gabon, where they were processed and stored at ambient temperature (20–30 °C) until analysis.

Obtaining Bark Extracts:-

Initially, the dried bark was ground into a fine powder using a mechanical grinder. Extraction was performed by decoction: precisely 100 g of bark powder were immersed in 1 L of distilled water and heated at 90 °C for 45 min**.** The resulting mixture was filtered through Whatman No. 1 filter paper (diameter: 10 cm). The filtrates obtained were dried in an oven at 60 °C until complete desiccation. The crude extracts were then stored at 4 °C until further analyses. Extraction yields were calculated as the ratio of the mass of dried crude extract obtained to the initial dry mass of plant material used

Phytochemical Screening:-

Preliminary phytochemical screening was performed on each aqueous extract to identify the major classes of secondary metabolites. The presence of these phytochemical groups provides a basis for the subsequent isolation of pharmacologically active compounds. The assays were conducted according to standard qualitative methods previously described by Harborne (1980) and Sofowora (1993) [23],[24]. Each test relied on the observation of characteristic color changes or precipitate formation following the addition of specific reagents. For accuracy, a control tube containing the same volume of solvent without extract was included for comparison in each assay.

Phenolic Compound Assays:-

Determination Of Phenol Content:-

The total polyphenol content of each aqueous extract was determined using the Folin–Ciocalteu colorimetric method with slight modifications [25]. The assay is based on the reduction of the Folin–Ciocalteu reagent by phenolic compounds, resulting in a blue complex measurable spectrophotometrically. Briefly, 0.25 mL of extract solution (1 mg/mL in distilled water) was mixed with 1.25 mL of Folin–Ciocalteu reagent. After 5 min of incubation at room temperature (25 ± 2 °C), 1 mL of 20% (w/v) sodium carbonate solution was added. The mixture was further incubated for 30 min at room temperature, and absorbance was recorded at 735 nm using a UV–visible spectrophotometer (Evolution 60S, Thermo Fisher Scientific, USA). Control tubes containing distilled water instead of extract were prepared in parallel. A calibration curve was established using gallic acid as the standard ($Y = 0.0012X - 0.0004$, $R^2 = 0.9902$), and total polyphenol content was expressed as milligrams of gallic acid equivalents per gram of dry extract (mg GAE/g extract).

Determination Of Flavonoid Content:-

The total flavonoid content of each extract was determined using the aluminum chloride ($AlCl_3$) colorimetric method with slight modifications [26]. This method is based on the formation of a stable complex between aluminum chloride and the keto or hydroxyl groups of flavonoids, producing a yellow coloration measurable spectrophotometrically. Briefly, 0.5 mL of 2% (w/v) $AlCl_3$ solution was mixed with an equal volume of extract diluted in methanol. After incubation for 10 min at room temperature (25 ± 2 °C), absorbance was measured at 415 nm using a UV–visible spectrophotometer (Evolution 60S, Thermo Fisher Scientific, USA) against a reagent blank. A calibration curve was established using quercetin as the standard ($Y = 0.0032X + 0.0077$, $R^2 = 1.0000$). Total flavonoid content was expressed as milligrams of quercetin equivalents per gram of dry extract (mg QE/g extract).

Determination of Tannin Content:-

The total tannin content of each extract was determined according to the European Community reference method for the determination of tannins [27]. This method is based on the formation of a colored complex between ferric ions and phenolic hydroxyl groups of tannins. Briefly, 0.25 mL of the extract was mixed with 1.25 mL of distilled water, 0.25 mL of ferric ammonium citrate solution (28% iron; 3.5 g/L, prepared 24 h in advance), and 1 mL of ammonia solution (8 g/L NH_3). The mixture was vortexed and incubated for 10 min at room temperature (25 ± 2 °C). Absorbance was then measured at 525 nm using a UV–visible spectrophotometer (Evolution 60S, Thermo Fisher Scientific, USA) against a reagent blank containing 200 µL of a mixture composed of 6 mL water, 1 mL ammonia, and 1 mL ferric ammonium citrate. A standard calibration curve was prepared using tannic acid ($Y = 0.0009X +$

0.2088; R^2 = 1.0000). Results were expressed as milligrams of tannic acid equivalents per gram of dry extract (mg TAE/g extract).

Determination of Proanthocyanidin Content:-

The total proanthocyanidin content of each extract was determined according to the method described by Prigent [28]. Briefly, 2.33 mL of a butanol/hydrochloric acid solution (70:30, v/v) was mixed with 0.16 mL of the extract in a test tube and vortexed for 1 min. The tubes were sealed with a layer of kerosene to prevent evaporation and heated in a water bath at 100 °C for 2 h. After cooling, 0.2 mL of the reaction mixture was used to measure absorbance at 550 nm using a UV–visible spectrophotometer (μQuant, BioTek Instruments Inc., USA) connected to KC Junior 1.31.5 software (BioTek Instruments Inc., USA). This method relies on the conversion of flavan-4-ols into anthocyanidins under acidic and thermal conditions, followed by the destruction of the newly formed pigments and partial elimination of chlorophyll derivatives during heating. Apple procyanidin (degree of polymerization = 7.4) purified by reverse-phase HPLC and characterized by thiol bond cleavage (kindly provided by Dr. Stéphanie Prigent, Wageningen University, Netherlands, and Dr. Catherine M.G.C. Renard, INRA Rennes, France) was used as the standard. A calibration curve was established using concentrations ranging from 0.5 μg/mL to 500 μg/mL. The proanthocyanidin content was expressed as milligrams of apple proanthocyanidin equivalents per gram of dry extract (mg APE/g extract). The standard curve equation was Y = 0.0006X + 0.0024 (R^2 = 0.9869).

Pharmacological Activities:-

Antioxidant Activity:-

DPPH Radical Scavenging Assay:-

The antioxidant activity of the extracts was assessed based on their ability to scavenge free radicals, specifically using the DPPH radical scavenging assay. This method is founded on the principle that DPPH, a stable free radical, exhibits a characteristic absorption band at 517 nm due to the resonance of its unpaired electrons. Upon reaction with an antioxidant compound, these unpaired electrons are stoichiometrically neutralized, forming products that absorb at 470 nm. Consequently, a decrease in absorbance at 517 nm reflects the discoloration of the DPPH solution and indicates radical scavenging activity. The assay was performed using a 10-tube microplate. In the first tube, 1.6 mL of methanol was mixed with 0.4 mL of extract solution prepared at a concentration of 1 mg/mL. To tubes 2 through 10, 1 mL of methanol was added, followed by serial dilutions in which 1 mL from each preceding tube was transferred to the next. Subsequently, 1 mL of DPPH solution (0.1 mg/mL) was added to each of the ten tubes. For the negative control, three blank tubes were prepared by mixing 1 mL of methanol with 1 mL of DPPH solution. A positive control was prepared as described by Ngoua **and al.** (2018) [29]. All samples were prepared in triplicate to ensure reproducibility. After incubation in the dark for 30 minutes, absorbance was measured at 517 nm using a spectrophotometer (Evolution 60S, USA) equipped with VISIONlite™ Version 5.1 software. The free radical scavenging activity was expressed as the percentage of DPPH reduced.

The percentage of inhibition (% Inhibition) was calculated using Equation (1):

$$\% \text{ Inhibition} = [(DO_{(}DPPH_{)} - DO_{sample}) / DO_{(}DPPH_{)}] \times 100$$

where $DO_{(}DPPH_{)}$ is the absorbance of the DPPH control solution and DO_{sample} is the absorbance of the test sample.

The concentration required to reduce 50% of the DPPH radicals (IC_{50}) was determined from the log–probit regression curve, obtained by plotting the free radical scavenging activity against the natural logarithm of the extract concentration [30]. In addition, the free radical scavenging activity index (IAA) was calculated to classify the antioxidant potential of the extracts [31].

The free radical scavenging activity index (IAA) was calculated according to Equation (2):

$$IAA = [DPPH] / IC_{50(}extract_{)}$$

where *[DPPH]* represents the concentration of the DPPH solution (50 μg/mL) and $IC_{50(}extract_{)}$ is the concentration of the extract required to inhibit 50% of DPPH radicals.

According to the classification criteria of Scherer and Godoy (2009), the antiradical activity of an extract is defined as follows [32]:

- **IAA < 0.5:** Low activity
- **0.5 ≤ IAA < 1:** Moderate activity
- **1 ≤ IAA < 2:** High activity
- **IAA ≥ 2:** Very high activity

Total Antioxidant Capacity:-

The total antioxidant capacity of the plant extracts was determined following the phosphomolybdenum method described by Kubola et al. (2008) [33], as applied by Ngoua et al. (2018). This assay is based on the reduction of molybdenum (VI) [Mo (VI)] to molybdenum (V) [Mo(V)] by the extract constituents under acidic conditions, resulting in the formation of a green phosphate/Mo(V) complex. Briefly, 0.3 mL of the extract dissolved in methanol was mixed with 3.0 mL of a reagent solution containing 0.6 mol/L sulfuric acid, 28 mmol/L disodium phosphate, and 4 mmol/L ammonium molybdate. The mixtures were incubated in a water bath at 70 °C for 90 min and then cooled to room temperature. The absorbance was recorded at λ = 695 nm using a spectrophotometer against a blank containing the vehicle solvent without extract. All samples were prepared in independent biological triplicates to ensure reproducibility. The total antioxidant capacity was calculated from two independent standard calibration curves established with quercetin and ascorbic acid (vitamin C), and results were expressed as milligrams of quercetin equivalents per gram of dry extract (mg QE/g extract) and milligrams of vitamin C equivalents per gram of dry extract (mg VCE/g extract), respectively.

Anti-inflammatory Activity:-

The anti-inflammatory activity was evaluated by protein denaturation method and membrane stabilization method, following the protocol of Ngoua and al**.** (2018) and Pavithra and al. (2025) [7, 47] with slight modifications.

Protein anti-denaturation test:-

The anti-inflammatory potential was evaluated by measuring the inhibition of bovine serum albumin (BSA) thermal denaturation, according to a method adapted from Williams et al. (2008) [35]. The reaction mixture, with a final volume of 3.0 mL, was prepared in separate test tubes by combining 0.1 mL of a 5% (w/v) BSA solution dissolved in phosphate-buffered saline (PBS, pH 6.4), 1.9 mL of PBS buffer, and 1.0 mL of plant extract or diclofenac sodium (used as a positive reference standard) at varying concentrations (0.0625, 0.125, 0.25, 0.5, and 1 mg/mL). Negative control tubes contained 0.1 mL of BSA solution, 1.9 mL of PBS, and 1.0 mL of distilled water.

To eliminate optical interference caused by the intrinsic coloration of the bark pigments, parallel sample blank tubes were systematically prepared for each concentration by replacing the BSA solution with an equivalent volume of PBS buffer. All tubes were gently homogenized and incubated at 37 °C for 20 min in an incubator (Ecocell, LSIS-B2V/EC55, Germany), then subjected to a thermal shock at 70 °C for exactly 5 min to induce protein aggregation. After cooling to room temperature, turbidity was quantified by measuring the optical density at λ = 660 nm using a UV-Visible spectrophotometer (Evolution 60S, USA). The net absorbance of each assay was determined by subtracting the absorbance of the corresponding sample blank from the test sample value. The percentage of protein stabilization, reflecting the inhibition of thermal denaturation, was calculated relative to the untreated negative control using Equation (1):

Inhibition (%) = [(Abs_control - Abs_net, sample) / Abs_control] × 100 (1):-

Where Abs_control represents the absorbance of the negative control and Abs_net, sample corresponds to the blank-corrected absorbance value of the sample or positive control. The extract concentration required to produce 50% inhibition (IC50) was determined from the log-probit dose–response curve.

Membrane stabilization test:-

The membrane stabilization test was evaluated by the method of hemolysis of red blood cells. This hemolysis was induced by heat.

Hemolysis induced by heat Samples of used extracts were dissolved in isotonic phosphate buffer solution. A set of 7 centrifugation tubes containing respectively 2 mL of extracts at increasing concentrations (29.76, 59.52, 119.04, 238.10, 476.19, and 952.38 µg/mL). Sodium diclofenac, with the same concentration range was used as the reference medicine. The negative control contained 2 mL of distilled water. A suspension of 0.1 mL of red blood cells was added to each of the tubes and mixed gently. The tubes were incubated at 54 °C for 20 min in a water bath. After incubation, tubes were centrifuged at 2500 rpm for 10 min at 4 °C and the hemoglobin content of the supernatant was estimated using the spectrophotometer (Evolution 60S, USA) at 540 nm.
The percentage of inhibition by the extract was calculated as follows:

% Inhibition of hemolysis = (1−ODsample/DOcontrol) x 100

Where OD sample = absorbance of the sample; DO control = absorbance of the control. The concentration of the extract for 50% inhibition (IC_{50}) was determined by the dose-response curve.

Anti-Sickling Activity:-

The **in vitro** evaluation of the antisicking activity of **E. chlorantha** and **A. boonei** extracts was carried out following the method of Emmel (1933) [36] , with minor modifications. Blood samples obtained from healthy volunteer donors carrying the heterozygous sickle cell trait (HbAS) were washed three times at 3,000 rpm for 5 minutes each to remove residual serum. Fifty microliters (50 µL) of washed red blood cells were incubated with a 2% sodium metabisulfite ($Na_2S_2O_5$) solution to induce sickling. Subsequently, 1 mL of physiological saline (0.9% NaCl) was added to each of three additional test tubes (tubes 2 to 4). In tube 1, 2 mL of plant extract (2 mg/mL) were introduced. A serial dilution was then performed by transferring 1 mL from tube 1 to tube 2, then from tube 2 to tube 3, and finally from tube 3 to tube 4, thereby generating a cascade dilution series. From each resulting concentration, 50 µL of extract were mixed with 50 µL of sickled red blood cells. The mixtures were placed between a microscope slide and coverslip, and the edges were sealed with clear, colorless varnish to prevent air entry. Four independent observations were made every 30 minutes for up to 120 minutes, and each experiment was performed in triplicate. Sickle cells and total erythrocytes were counted across ten microscopic fields. Erythrocyte morphology was analyzed using an immersion microscope (Motic Digital Microscope, B1 Advanced Series) connected to a computer equipped with MI Devices software. Both the percentage of sickled cells and the reversibility of sickling were assessed in each field. Hydroxyurea was used as the positive control, and physiological saline served as the negative control.

The percentage of sickled cells (F) was calculated using Equation (1):

$$F\ (\%) = (ND / NT) \times 100$$

where **ND** is the number of sickled cells and **NT** is the total number of red blood cells.

The normalization rate (R) for each concentration was determined using Equation (2):

$$R\ (\%) = [(F_0 - F_n) / F_0] \times 100$$

Where F_0 represents the initial percentage of sickled cells in the negative control and F_n is the percentage of sickled cells at a given extract concentration. For a blood sample to be considered valid, the sickling ratio must be ≥ 80 ± 5%.

In-Vitro Blood Anticoagulant Activity:-

The **in vitro** anticoagulant activity was evaluated according to the method of Lee and White (1913) [37], as modified by Ramdé-Tiendrébéogo **and al.** (2014) [38] , with minor adjustments. A sample of freshly collected venous blood obtained from **six (N = 6) healthy donors, without distinction of their specific hemoglobin genotype**, was utilized for the whole-blood clotting assay. Timing began immediately upon blood collection. Eight glass tubes, prerinsed with physiological saline and air-dried, were labeled from 1 to 8. One milliliter (1 mL) of physiological saline (0.9% NaCl) was added to tubes 2 through 8. Two milliliters (2 mL) of extract solution (20 mg/mL) were introduced into tube 1, and a serial dilution was performed by transferring 1 mL sequentially from tube 1 to tube 8. A corresponding mixture containing 1 mL of physiological saline instead of extract served as the negative control. The tubes were capped with sterile cotton plugs and immediately placed in a water bath (Buchi, Switzerland) maintained at 37 °C without agitation. After 3 minutes, the tubes were removed and gently tilted at a 45° angle to check for coagulation. In the absence of clot formation, the tubes were returned to the water bath and examined every 30 seconds until coagulation occurred (i.e., no flow was observed when the tube was inverted). The coagulation time was recorded for each tube once the first signs of clot formation appeared. Extracts of **E. chlorantha** and **A. boonei** were evaluated following this same procedure.

Statistical Analysis:-

Data were compiled and organized using Microsoft Excel 2010 and Python 3.13 for statistical analysis. Qualitative (nominal) variables are presented as absolute frequencies and percentages (%), whereas quantitative variables are expressed as arithmetic mean ± standard deviation (SD). The number of independent biological replicates was defined as N = 2 for the anti-sickling screening (using erythrocytes derived from two separate HbAS donors) and N = 6 for the whole-blood clotting time experiment (derived from six independent healthy donors). For spectrophotometric antioxidant and anti-inflammatory assays, results are based on three independent experiments (N = 3). In all experimental models, each individual sample was analyzed in technical triplicates (n = 3). Half-maximal inhibitory concentrations (IC_{50}) were estimated by non-linear or log-probit regression analysis with 95% confidence intervals. Statistical assumptions of normality and homoscedasticity were verified prior to executing one-way analysis of variance (ANOVA), followed by Tukey's post hoc test for multiple comparisons. Statistically significant differences between experimental groups are indicated by distinct lowercase letters or asterisks above the bars ($p < 0.05$).

Results and Discussion:-

Results of Phytochemical Screening:-

Phytochemical screening results for *A. boonei* ***and*** *E. chlorantha* are summarized in **Table 1**. The table reports the relative presence of major compound classes, as determined through standardized phytochemical assays, thereby providing a comparative overview of the chemical profiles of the two species**.**

Chemical analysis of the aqueous extracts of ***E. chlorantha*** and ***A. boonei*** revealed the presence of significant amounts of bioactive compounds. Both extracts contained high levels of saponins, polyphenols, tannins, cyanidins, coumarins, and reducing sugars. In addition, the aqueous extract of ***A. boonei*** was particularly rich in alkaloids and cardiotonic glycosides, whereas the extract of ***E. chlorantha*** showed a high content of proanthocyanidins. The presence of these phytoconstituents supports the traditional medicinal use of these plants in the management of various ailments, including sickle cell anemia, malaria, body pain, wound infections, nausea, jaundice, fever, splenic disorders in children, hepatitis, intestinal worms, gastrointestinal spasms, sexual weakness, urinary infections, typhoid fever, leprosy lesions, tuberculosis, gastric and duodenal ulcers, and diarrhea. These findings are consistent with previous reports by Tcheghebe **and al.** (2016) and Olanlokun and Olorunsogo (2018) [14],[15],[19],[20].

Table 1 : Phytochemical screening results

Chemical groups	*Alstonia boonei* De Wild	*Enantia chlorantha* Oliv
Saponins	+++	+++
Polyphenols	+++	+++
Sterols and Triterpenes	-	-
Simple sugars and Holosides	+	-
Tannins	+++	++
Alkaloids	+++	+
Cyanidins	+++	+++
Total flavonoids	+	-
Anthocyanins	+	+
Proanthocyanidins	+	++
Anthracenics	+	+
Coumarins	+++	+++
Cardiac glycosides	++	-
Reducing sugars	+++	++
Iridoids	++	++

Legend : +++ very abundant, ++ abundant, + less abundant, - absent

Determination of bioactive compounds and extraction yield in aqueous extracts:-

The aqueous extraction yields of ***E. chlorantha*** and ***A. boonei*** were 6.22% and 4.50%, respectively. The higher yield obtained from ***E. chlorantha*** may be attributed to several factors, including differences in harvesting methods, plant origin, varietal characteristics, season of collection, climatic and environmental conditions, geographical location, disease status, plant maturity, and storage duration. Indeed, the two plant samples were collected from distinct localities, which could have influenced both the quality and the quantity of the extracted materials. Madiélé and al. (2015) reported comparable findings for ***E. chlorantha***, with an aqueous extract yield of 7.32%, confirming the similarity in extraction efficiency [39]. The total phenolic content ranged from 41.58 ± 0.75 mg GAE/g for ***E. chlorantha*** to 67 ± 1.58 mg GAE/g for ***A. boonei***. The total flavonoid content was 341.1 ± 6.77 mg QE/g for ***E. chlorantha*** and 79.93 ± 11.60 mg QE/g for ***A. boonei***. Proanthocyanidin contents were 2.67 ± 0.40 mg APE/g for ***E. chlorantha*** and 7.67 ± 2.64 mg APE/g for ***A. boonei***. Overall, ***A. boonei*** exhibited higher levels of total phenolics and proanthocyanidins, whereas ***E. chlorantha*** showed a markedly higher flavonoid content.

Table 2 : Extraction yields and quantitative phytochemical composition of the bark extracts

Extracts	Extraction yield (%)	Total phenolic content (mg GAE/g)	Total flavonoid content (mg QE/g)	Proanthocyanidin content (mg APE/g)
ECO	6.22	41.58 ± 0.75	341.10 ± 6.77	2.67 ± 0.40
ABW	4.50	67.00 ± 1.58	79.93 ± 11.60	7.67 ± 2.64

Note: *ECO, Enantia chlorantha aqueous extract; ABW, Alstonia boonei aqueous extract. Values are expressed as mean ± standard deviation (N = 3 independent experiments). GAE = gallic acid equivalents; QE = quercetin equivalents; APE = apple proanthocyanidin equivalents.*

Pharmacological Activity:-

Radical scavenging kinetics and total net reductive capacity

Aqueous Extracts (ABW & ECO Phenolics)
- ⟶ High Molecular Weight Matricies ⟶ Steric Hindrance ⟶ Slow HAT Kinetics (High IC50)
- ⟶ Polyhydroxyl/Reducing Frameworks ⟶ Positive Mo(VI) → Mo(V) Electron Transfer

The screening of radical scavenging kinetics via the DPPH assay highlighted distinct behaviors between the crude bark extracts and the pure reference standards (Figure 1). The mathematical resolution of the IC_{50} curves (Figure 1, Panel A) gave values of 195.81 ± 1.94 µg/mL for *Alstonia boonei* (ABW) and 600.02 ± 3.37 µg/mL for *Enantia chlorantha* (ECO). One-way ANOVA confirmed that these differences across the experimental groups are highly significant ($p < 2.2 \times 10^{-16}$). These values are higher than those of the low-molecular-weight reference molecules, namely quercetin (11.22 ± 0.61 µg/mL), BHT (13.76 ± 0.03 µg/mL), and vitamin C (4.60 ± 0.10 µg/mL).

From a structural perspective, this slower scavenging rate is not due to a lack of active chemical groups, but rather to steric hindrance and molecular size. Crude aqueous decoctions from woody barks are rich in high-molecular-weight condensed tannins (proanthocyanidins) and glycosylated frameworks, as established by Harborne (1998) [23]. When reacting with a stable, hindered radical like DPPH, these large polyphenolic structures experience limited spatial access to the radical core. This slows down their Hydrogen Atom Transfer (HAT) and Single Electron Transfer (SET) pathways compared to small, agile reference standards like vitamin C or quercetin.

This structural mechanism is supported by the phosphomolybdenum assay, which measures total antioxidant capacity via a net electron transfer process (Mo(VI) → Mo(V)) (Figure 1, Panels C and D). Both extracts successfully reduced the phosphomolybdate complex. Specifically, Alstonia boonei exhibited a significantly higher overall reducing capacity than Enantia chlorantha across both calibration standards, yielding 3.80 ± 0.79 mg QE/g versus 1.26 ± 0.25 mg QE/g (Panel C, $p < 2.2 \times 10^{-16}$), and 0.81 ± 0.62 mg VCE/g versus 0.65 ± 0.56 mg VCE/g (Panel D, $p = 1.7 \times 10^{-5}$). In the pathophysiology of sickle cell disease, chronic oxidative stress is a primary driver of erythrocyte damage, lipid peroxidation, and vaso-occlusive crises [40]. The oxidation of intra-erythrocytic iron ($Fe^{2+} \rightarrow Fe^{3+}$) destabilizes the cell membrane, accelerating sickle-cell distortion and endothelial adhesion [41]. While the *in vitro* DPPH kinetics of ABW and ECO appear slow due to these structural parameters, their total net reducing power is biologically valuable. Their therapeutic effects observed *in vivo* likely stem from alternative pathways. These include the non-specific complexation of target proteins, membrane stabilization, or the modulation of vascular inflammatory signals, rather than simple free radical scavenging [42,43].

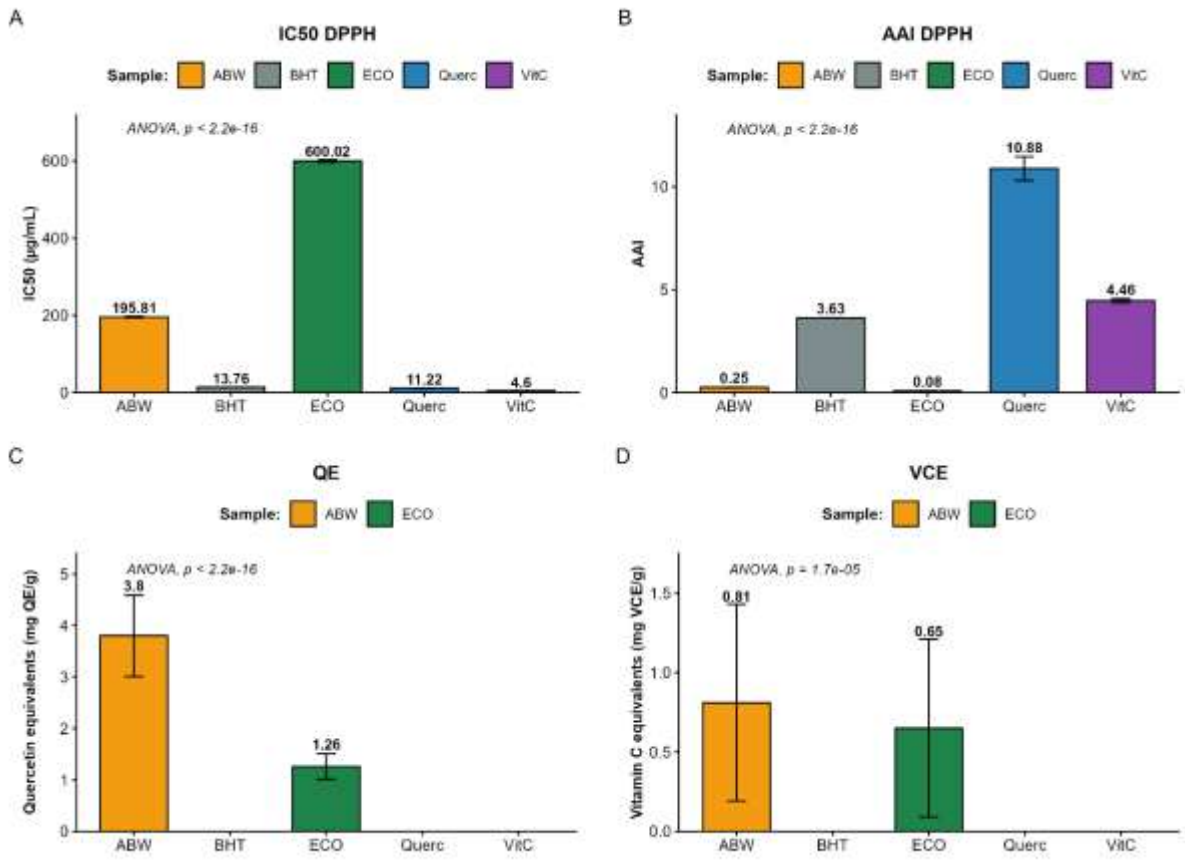


Figure 1: *In vitro* antioxidant profiles of *Alstonia boonei* (ABW) and *Enantia chlorantha* (ECO) aqueous bark extracts. **Panel (A):** Radical scavenging half-maximal inhibitory concentrations (IC_{50}, µg/mL) of *E. chlorantha*, *A. boonei*, vitamin C, BHT, and quercetin determined by the DPPH assay. **Panel (B):** Antioxidant Activity Index (AAI) derived from the DPPH radical scavenging assay. **Panel (C):** Total antioxidant capacity expressed as milligrams of quercetin equivalents per gram of dry extract (mg QE/g) determined by the phosphomolybdenum assay. **Panel (D):** Total antioxidant capacity expressed as milligrams of vitamin C equivalents per gram of dry extract (mg VCE/g) determined by the phosphomolybdenum assay. Data are presented as mean ± standard deviation (SD) from three independent experiments ($N = 3$, technical triplicates $n = 3$). Statistical annotations denote highly significant overall variations ($p < 0.001$) according to one-way analysis of variance (ANOVA). ABW: *Alstonia boonei* De Wild (yellow); ECO: *Enantia chlorantha* Oliv. (green); Querc: quercetin (blue); VitC: vitamin C (purple); BHT: butylated hydroxytoluene (gray); QE: quercetin equivalents; VCE: vitamin C equivalents. Linear regression equations for DPPH curves: *E. chlorantha* ($y = 0.0865x - 1.902$, $R^2 = 0.995$); *A. boonei* ($y = 0.3484x - 18.22$, $R^2 = 0.983$).

Anti-Inflammatory Activity:-

Evaluation of Anti-Inflammatory Activity by Albumin Denaturation and membrane stabilization test:-

Vaso-occlusive crises and microvascular blockages in sickle cell disease are heavily driven by chronic cellular activation and secondary tissue inflammation [6,41]. To evaluate the protective potential of the Gabonese bark decoctions against tissue and cellular damage, two complementary in vitro models were used: heat-induced erythrocyte hemolysis (AIME) and albumin anti-denaturation (BE) (Figure 2).

Aqueous Extracts (Flavonoids) ┌──► Erythrocyte Membrane (AIME) ──► Membrane Intercalation ──► Low IC50 (65.4 - 77.3 µg/mL)

└──► Albumin Protection (BE) ──► Hydrophobic H-Bonding ──► Parallels Diclofenac (~450 µg/mL)

The heat-induced hemolysis assay (Figure 2, Panel A, left) showed a strong protective effect for both plant extracts, outperforming the standard non-steroidal anti-inflammatory drug (NSAID). *Enantia chlorantha* (ECO) and *Alstonia boonei* (ABW) stabilized human erythrocyte membranes at low concentrations, showing IC_{50} values of 65.4 µg/mL and **77.3**µg/mL respectively. One-way ANOVA confirmed highly significant differences across the groups ($p = 3.1 \times 10^{-6}$).

Tukey's post hoc comparisons showed that both crude extracts significantly outperformed diclofenac sodium (IC_{50} = 337.57 ± 23.48 µg/mL, $p < 0.001$), while no statistical difference was observed between ECO and ABW ($p > 0.05$). As shown in the dose-response profiles (Panel B), membrane protection followed a clear concentration-dependent trend.

In the protein anti-denaturation model (Panel A, middle), the extracts matched the performance of the clinical standard. The calculated IC_{50} values were 419.5 µg/mL for ABW, 454.1 µg/mL for ECO, and 461.7 ± 42.09 µg/mL for diclofenac sodium. The overall ANOVA revealed no significant variations among these three groups ($p = 0.62$), showing that the complex plant extracts protect the tertiary structure of proteins as effectively as the purified drug.
From a structural perspective, these dual anti-inflammatory properties are closely linked to the alkaloids, flavonoids, and saponins identified in the quantitative profiling (Table 2). The massive presence of core flavonoid frameworks in *E. chlorantha* (341.10 ± 6.77 mg QE/g) and condensed tannins in *A. boonei* provides a high density of aromatic rings and polar hydroxyl branches. These active structures can form hydrogen-bonding net networks with the hydrophobic pockets of serum proteins, preventing thermal unfolding [28].

Additionally, the amphiphilic structure of saponins allows them to sit within the lipid bilayer of erythrocytes, stabilizing the cell membrane against thermal lysing without altering internal osmotic volume [44]. This multi-site protection explains their high anti-inflammatory action despite their slow direct radical scavenging kinetics.

In sickle cell disease, this dual mechanism can help limit vascular wall irritation, reduce endothelial adhesion, and support microvascular blood flow [3,45]. However, translating these findings into safe clinical uses requires careful dosage management.

While *E. chlorantha* maintains a wide safety window in animal models up to 500 mg/kg [14,15], *A. boonei* requires strict concentration monitoring. Its alkaloid fraction can cause dose-dependent hepatotoxic and nephrotoxic injuries at chronic systemic doses near or exceeding 400 mg/kg [22].

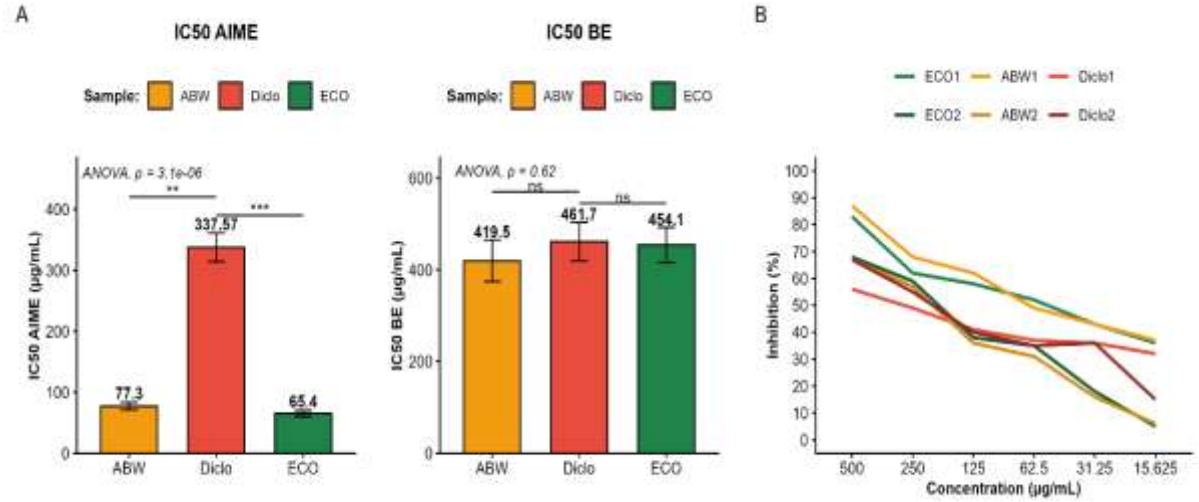


Figure 2: Evaluation of bio-macromolecular and cellular membrane stabilization by *Alstonia boonei* (ABW) and *Enantia chlorantha* (ECO) aqueous bark extracts. **Panel (A):** Half-maximal inhibitory concentrations (IC_{50}, µg/mL) for heat-induced erythrocyte hemolysis (AIME, left) and bovine serum albumin thermal anti-denaturation (BE, middle). **Panel (B):** Dose-dependent inhibition profiles (%) across tested concentrations (15.625 to 500 µg/mL), where ECO1, ABW1, and Diclo1 represent erythrocyte hemolysis inhibition, and ECO2, ABW2, and Diclo2 represent albumin thermal denaturation inhibition. Data are presented as mean ± standard deviation (SD) from three

independent experiments ($N = 3$, technical triplicates $n = 3$). Asterisks denote statistical significance levels (** $p < 0.01$, *** $p < 0.001$, ns: not significant, $p > 0.05$) derived from one-way ANOVA followed by Tukey's post hoc test. Diclofenac sodium (Diclo) served as the reference anti-inflammatory standard. ABW: *Alstonia boonei* De Wild (yellow); ECO: *Enantia chlorantha* Oliv. (green); Diclo: diclofenac sodium (red).

Anti-coagulant activity of *Alstonia boonei De Wild* and *Enantia chlorantha* extracts:-

The physiological baseline blood clotting time of the sampled human cohorts, in the absence of exogenous plant materials, spanned from (6.02 ± 0.58) to (9.74 ± 2.36) min (Figure 3, 0 µg/mL control baseline). This intrinsic window reflects individual fluctuations in hemoglobin genotypes among the donors.

Individuals expressing sickle cell traits (homozygous SS or heterozygous SC) exhibit accelerated baseline clot progression due to cell-surface distortions, circulating micro-aggregates, and hypercoagulable states, as previously demonstrated by Ramdé-Tiendrébéogo and al. (2019) [46].

ECO Extract (Hyper-coagulation) ⟶ Massive Flavonoid Loading ⟶ Alteration of Fibrin Clot Elasticity

ECO Extract (Hyper-coagulation) ⟶ Isoquinoline Alkaloid Core ⟶ Steric Blockade of Thrombin Sites

The introduction of *A. boonei* (ABW) and *E. chlorantha* (ECO) aqueous extracts altered this pathway in a dose-dependent manner. At concentrations between 125 and 10,000 µg/mL, clot matrix assembly was delayed beyond the clotting intervals of the untreated controls.

At the highest tested concentration (10,000 µg/mL), anticoagulation times extended to 33.08 ± 7.81 min for ABW and reached a peak of 45.32 ± 2.59 min for ECO, demonstrating a highly significant overall variance between the two species ($p < 0.001$).

The superior anticoagulant efficacy demonstrated by *E. chlorantha* over *A. boonei* corresponds with the quantitative chemometric profiles established in Table 2. As shown in our quantitative assays, *E. chlorantha* has a high total flavonoid content (341.10 ± 6.77 mg QE/g), which is more than four times higher than that of *A. boonei*.

From a structure-activity perspective, these specialized polyhydroxyl structures and alkaloid cores previously reported in the literature for these species (such as palmatine, berberine, or echitamine) [12,14,17] may interact via non-covalent networks [46].

Furthermore, the polar saponins present in both bark extracts (Table 1) act as natural amphiphilic surfactants. These molecules can embed within the cell membrane or form a steric barrier around polymerizing fibrin strands. This dual mechanism delays thrombin cleavage and slows the conversion of fibrin monomers into rigid clot structures [10].

In managing sickle cell disease, reducing hypercoagulability is critical for preventing thromboembolic complications and vaso-occlusive crises triggered by rigid, sickled red blood cells [6]. These findings suggest that the aqueous bark extracts of *E. chlorantha* and *A. boonei* can serve as natural anticoagulant agents. They help mitigate the risk of microvascular blockages without requiring single-compound synthetic therapies [11]

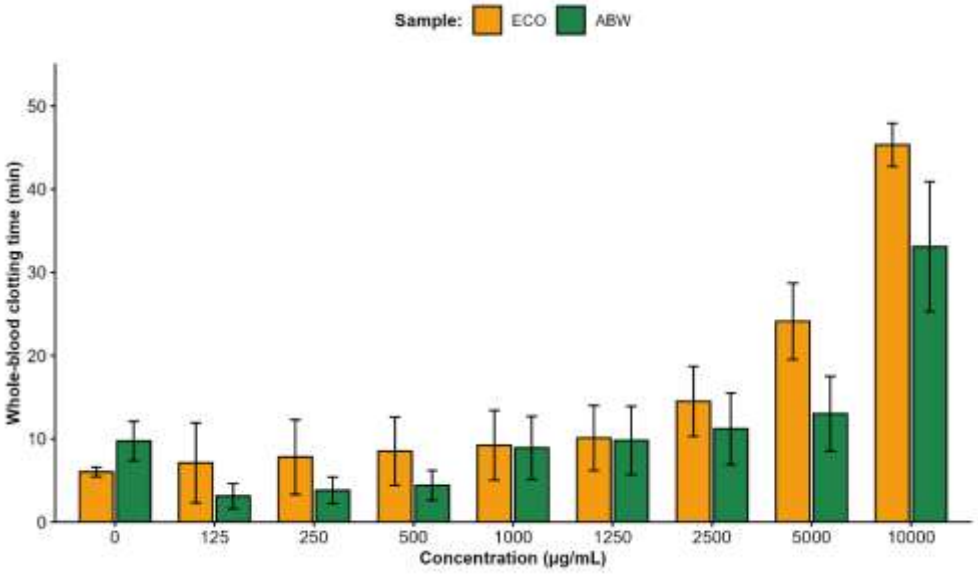


Figure 3: *In vitro* dose-dependent prolongation of whole-blood clotting times by *Enantia chlorantha* (ECO) and *Alstonia boonei* (ABW) aqueous bark extracts across a concentration gradient (125 to 10,000 µg/mL) using the Lee–White method. Data are expressed as mean ± standard deviation (SD) from six independent healthy donors ($N = 6$, technical triplicates $n = 3$). Statistically significant differences between the two plant extracts become prominent at higher concentrations ($p < 0.001$), as determined by one-way ANOVA followed by Tukey's post hoc test. Baseline physiological clotting times (0.9% NaCl negative control, absence of extract) are plotted at the 0 µg/mL mark. ECO: *Enantia chlorantha* Oliv. (yellow); ABW: *Alstonia boonei* De Wild (green).

Molecular mechanism of anti-sickling kinetics and erythrocyte phenotypic normalization:-

The phenotypic distortion of human erythrocytes under chemical hypoxia represents the terminal structural hallmark of hemoglobin S (HbS) polymerization. Exposing AS red blood cells to a 2% sodium metabisulfite ($Na_2S_2O_5$) solution successfully lowered the partial oxygen pressure (pO_2), triggering HbS deoxygenation and self-assembly.

Under basal conditions (Negative Control), the baseline percentage of sickled erythrocytes expanded progressively over time, rising from 80.81 ± 1.95% at 0.5 h to a peak of 89.10 ± 2.11% after 2 h. This time-dependent kinetic behavior matches the stabilization of the tense (T) state of the HbS tetramer, which exposes a hydrophobic pocket involving Val-6 that accelerates polymer nucleation [47]. This severe structural distortion is visually confirmed by optical microscopy, showcasing a predominant proportion of rigid, elongated, and spiculed sickle phenotypes. These indices closely agree with the baseline values (0.85 ± 0.09) described by Lokonon and al. (2021) using equivalent chemical triggers [48] Figure 4.

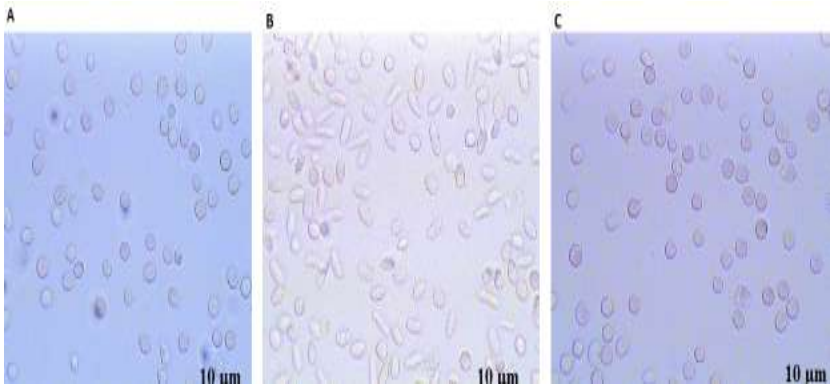


Figure 4: Representative optical micrographs (100× magnification) of human heterozygous sickle cell trait (HbAS) erythrocyte morphological transitions under controlled chemical hypoxia (N = 2 independent donors).

Panel (A): Normoxic physiological control (0.9% NaCl) showing normal biconcave discocyte morphology.
Panel (B): Sickled erythrocytes induced by 2% sodium metabisulfite ($Na_2S_2O_5$) after 2 h of incubation under basal hypoxic conditions (negative control without extract), displaying rigid, elongated, and spiculed phenotypes.
Panel (C): Hypoxic erythrocytes treated with the reference drug hydroxyurea (1,000 µg/mL) after 2 h, exhibiting partial morphological restoration. Scale bar = 10 µm.

[Negative Control] ⟶ Baseline sickling accelerates over time, peaking at 89.1%
[Hydroxyurea] ⟶ High dose (1000 µg/mL) increases slowly to 52.26%; low dose decays to 11.52% [Plant Extracts] ⟶ Dose- and time-dependent acceleration, peaking at ~75.4% at 2 h

The positive control, hydroxyurea, displayed an atypical, dose-dependent kinetic inversion over time. At its lowest tested concentration (125 µg/mL), its capacity to reverse sickling collapsed significantly during the assay, dropping from an initial 43.60% at 0.5 h down to a minimal 11.52% at 2 h. Conversely, at its highest concentration (1000 µg/mL), hydroxyurea required the full 2 h incubation period to reach its maximum reversibility of 52.26%.

In clinical practices, hydroxyurea acts as a systemic antimetabolite that mitigates vaso-occlusive crises by inducing fetal hemoglobin (HbF, $\alpha_2\gamma_2$) synthesis within bone marrow erythroid progenitors [49]. In an ex vivo acellular setup using washed erythrocytes, this transcriptional pathway is non-functional. Therefore, the observed delay and limited ex vivo performance emphasize that single-target antimetabolites lack immediate polymer-disrupting efficiency

when subjected to acute, direct chemical hypoxia in mature erythrocytes, a phenomenon further complicated by known pharmacokinetic variations in systemic profiles [46].

In sharp contrast, the aqueous bark extracts of *Alstonia boonei* (ABW) and *Enantia chlorantha* (ECO) exerted a powerful, concentration-dependent, and chronologically stable anti-sickling effect. At the minimum concentration of 125 µg/mL maintained over 2 h, the percentage of reversibility reached 49.37% for ABW and 57.30% for ECO. When the concentration was raised to 1000 µg/mL, both Gabonese plants achieved their maximum therapeutic effect, yielding closely matched and stable restoration values of 75.44% (ABW) and 75.23% (ECO) at the 2 h threshold, significantly outclassing the reference drug under identical hypoxic stresses[17,42,43] Figure 5.

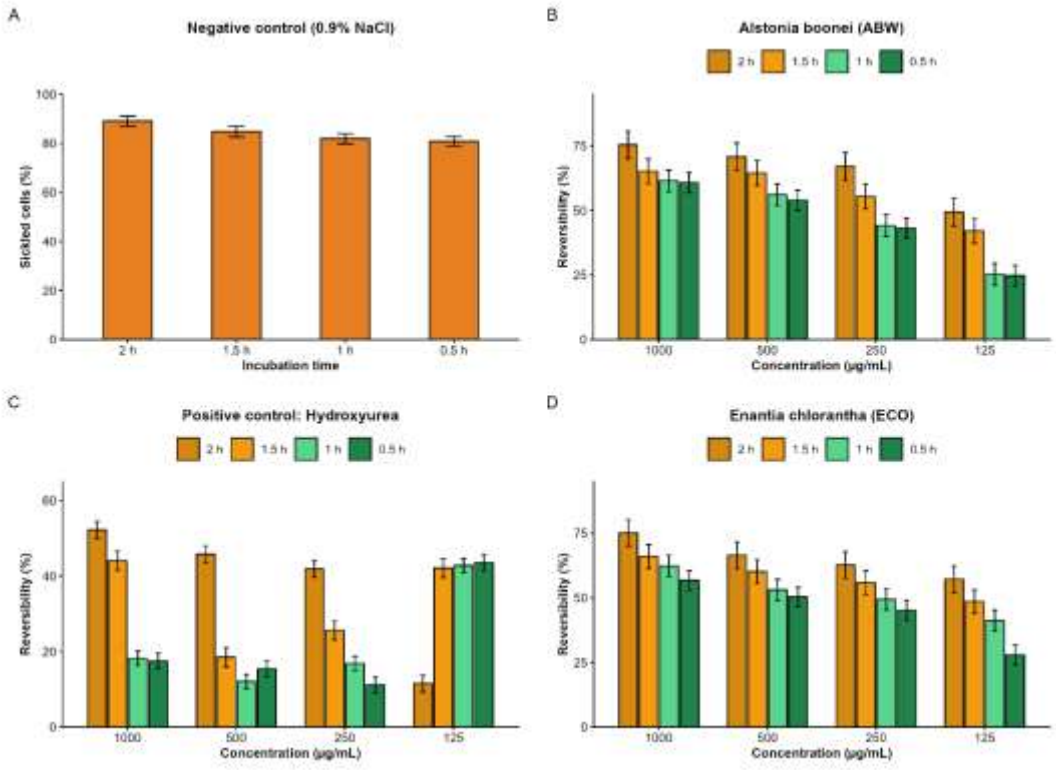


Figure 5: *In vitro* kinetic resolution of anti-sickling and HbAS erythrocyte reversibility profiles over a 2 h incubation period under 2% $Na_2S_2O_5$-induced chemical hypoxia. **Panel (A):** Negative control (0.9% NaCl) showing the progressive time-dependent increase in the percentage of sickled cells without treatment. **Panel (B):** Concentration- and time-dependent percentage of sickling reversibility induced by *Alstonia boonei* (ABW) aqueous bark extract (125 to 1,000 µg/mL). **Panel (C):** Kinetic profiles of the positive control (hydroxyurea, 125 to 1,000 µg/mL), showing a dose-dependent variation over time. **Panel (D):** Concentration- and time-dependent percentage of sickling reversibility induced by *Enantia chlorantha* (ECO) aqueous bark extract (125 to 1,000 µg/mL). Data are expressed as mean ± standard deviation (SD) from two independent HbAS donors (N = 2, technical triplicates n = 3). Time intervals are standardized to decimal notation (0.5 h, 1 h, 1.5 h, and 2 h).

The direct ex vivo dynamic of this herbal synergy is visually trackable through the chronological microscopic monitoring of the treated erythrocytes. During the initial phase of incubation (30 min), the erythrocyte matrix remains dominated by highly distorted and sickle-shaped architectures, confirming that chemical oxygen depletion operates at a faster initial velocity than the passive transmembrane influx of the polar phytoconstituents.

However, a major morphological shift is visible from 1 h to 1 h 30 min, where the proportion of falciform shapes decreases significantly, giving way to transitional, softened erythrocyte envelopes. At the 2 h terminal benchmark, the erythrocyte pool achieves a complete phenotypic normalization, showing a total recovery of healthy circular, biconcave, and highly flexible geometry Figure 6.

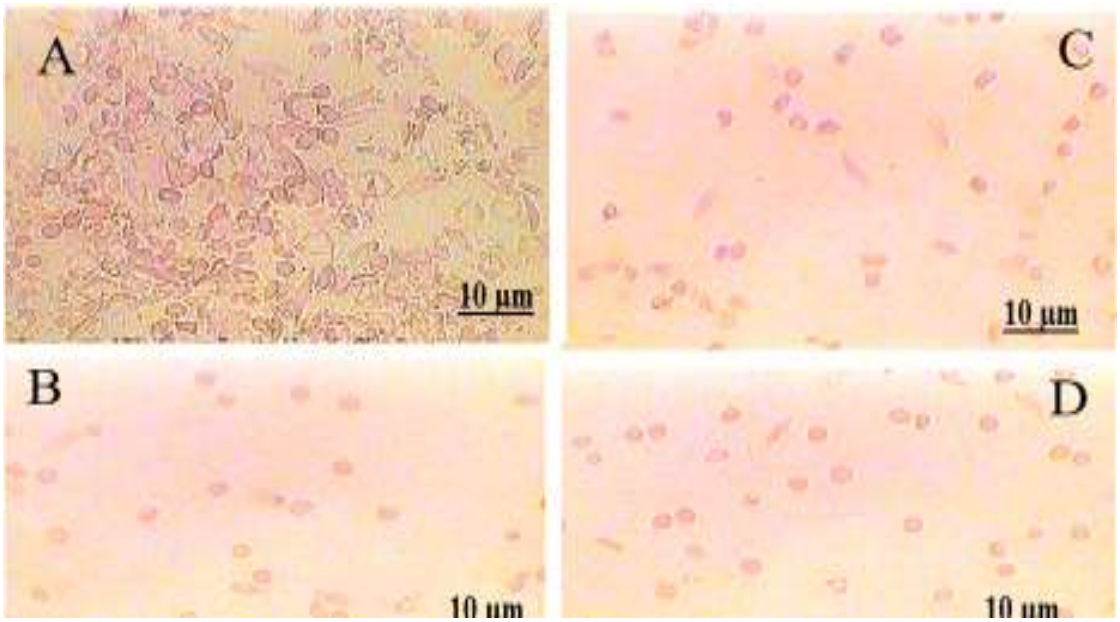


Figure 6: Optical micrographs (100× magnification) illustrating the time-dependent phenotypic normalization of human HbAS erythrocytes treated with crude **Enantia chlorantha** aqueous bark extract (1,000 µg/mL) under 2% $Na_2S_2O_5$-induced chemical hypoxia (**N** = 2 independent donors).
Panel (A): Cellular state after 0.5 h of incubation, showcasing a predominant proportion of rigid, elongated sickle phenotypes.
Panel (B): Incubation state after 1 h, showing initial structural reversion transitions.
Panel (C): Incubation state after 1.5 h, characterized by progressive depletion of sickled cells. **Panel (D):** Terminal state after 2 h, exhibiting maximal morphological restoration toward typical, flexible biconcave erythrocytes. Scale bar = 10 µm.

From a strict phytochemistry perspective, this time-dependent reversion sequence confirms that the therapeutic action of *E. chlorantha* and *A. boonei* relies on a diffusion-controlled macromolecular interaction [12,17,29,50]. The highly water-soluble flavonoid glycosides dominant in ECO and the polar monoterpene indole alkaloids characteristic of ABW cross the cell boundary via passive transport.

As incubation time progresses, these molecules accumulate in the cytoplasm, allowing them to effectively saturate the inter-tetramer contact nodes of deoxygenated HbS. By outcompeting the hydrophobic alignment of the abnormal Val-6 residues, this complex plant mixture halts polymer nucleation over time, a protective mechanism shared by other highly concentrated African medicinal extracts [27].

The extensive screening confirms that this anti-sickling effect is supported by water-soluble anthocyanins, polar saponins, and reducing sugars which actively stabilize the erythrocyte lipid membrane [27]. Furthermore, specific alkaloidal scaffolds including *echitamine* and *alstonine* previously isolated from the bark of *A. boonei* play a major role in blocking hemoglobin assembly [12,17], whereas specialized single molecules like phenylalanine, p-hydroxybenzoic acid derivatives, and core triterpenoids (such as maslinic, oleanolic, and betulinic acids) may offer parallel multi-site protection [29,50].

Consequently, the water-soluble extracts of *E. chlorantha* and *A. boonei* act as multi-target anti-sickling complexes, making them highly promising candidates for developing affordable phytomedicines to manage sickle cell disease in sub-Saharan Africa.

To establish a verified baseline of therapeutic efficacy, a direct comparative screening of the anti-sickling reversibility was resolved across a fixed concentration gradient (Figure 7).

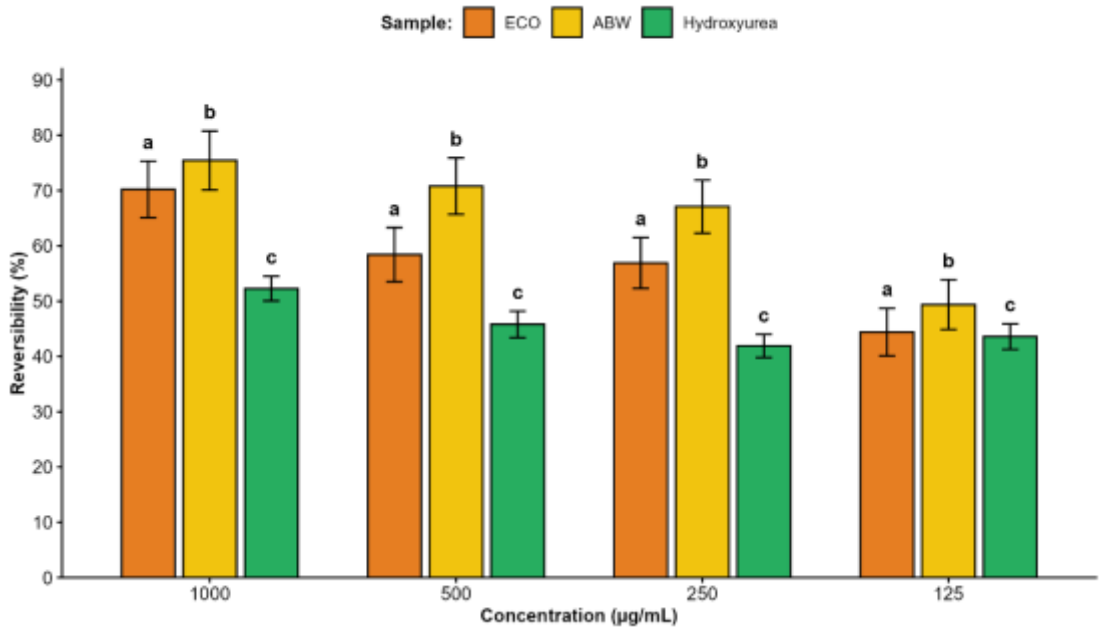


Figure 7: Comparative *in vitro* anti-sickling screening and phenotypic normalization rates of *Enantia chlorantha* (ECO), *Alstonia boonei* (ABW), and hydroxyurea across a concentration gradient (125 to 1,000 µg/mL) after 2 h of incubation under 2% $Na_2S_2O_5$-induced chemical hypoxia. Data are presented as mean ± standard deviation (SD) from two independent HbAS donors (N = 2, technical triplicates n = 3). Different lowercase letters (a, b, c) above the bars at each concentration indicate statistically significant differences between treatments ($p < 0.05$), as determined by one-way ANOVA followed by Tukey's post hoc test. ECO: *Enantia chlorantha* Oliv. (orange); ABW: *Alstonia boonei* De Wild (yellow); hydroxyurea (green).

[1000 µg/mL] ⟶ ABW (75.44%, b) ⟶ ECO (70.21%, a) ⟶ Hydroxyurea (52.26%, c) [125 µg/mL] ⟶ ABW (49.37%, b) ⟶ ECO (44.40%, a) ⟶ Hydroxyurea (43.60%, c)

The quantitative distribution of phenotypic normalization rates demonstrates a highly significant, dose-dependent superiority of both Gabonese crude bark extracts over the reference drug. At the highest tested concentration (1000 µg/mL), *Alstonia boonei* (ABW) reached the highest overall reversibility percentage (75.44 ± 5.34%, label b), followed closely by *Enantia chlorantha* (ECO) at 70.21 ± 5.12%, label a), while hydroxyurea plateaued significantly lower at 52.26 ± 2.22%, label c).

This statistical hierarchy (ABW > ECO > hydroxyurea) remains prominent across the entire concentration range down to 125 µg/mL, as validated by Tukey's multiple comparison test ($p < 0.05$), confirming the distinct anti-sickling pathways of these agents.

While hydroxyurea is the gold standard for reducing vaso-occlusive crises in vivo by inducing fetal hemoglobin (HbF) synthesis, its limited efficacy in this acute, acellular setup (52.26 ± 2.22%) is expected, as mature erythrocytes lack transcriptional machinery. Therefore, the observed outperformance by the crude extracts underscores a direct, non-transcriptional membrane or macromolecular interaction, rather than clinical superiority over hydroxyurea.

In contrast, the immediate and sustained action of the complex plant matrices stems from a direct diffusion-controlled macromolecular interaction. The high accumulation of specialized polyhydroxyl flavonoids and condensed tannins in ECO and ABW provides a highly active pool of chemical rings. These natural structures pass through the erythrocyte membrane and physically bind into the hydrophobic docking cavities of the deoxygenated HbS tetramers, blocking polymer nucleation without requiring internal cell transcription mechanisms.

Simultaneously, the active presence of specialized triterpenoids and plant secondary metabolites helps maintain outer membrane fluidity, preventing cellular lysis under severe chemical stress. From a structure-activity perspective, these specialized polyhydroxyl structures and alkaloid cores previously reported in the literature for

these species (such as palmatine, berberine, or echitamine) [12,14,17] may interact via non-covalent networks, thereby halting polymer nucleation and stabilizing the erythrocyte architecture. These chemometric results confirm that the traditional aqueous decoctions of E. chlorantha and A. boonei act as multi-target anti-sickling complexes, making them promising candidates for developing affordable and effective treatments for sickle cell disease.

Limitations of the Study:-

Although the current findings demonstrate promising preliminary in vitro antioxidant, anti-inflammatory, antisickling, and anticoagulant properties, several limitations must be acknowledged. First, the evaluation was strictly restricted to acellular and ex vivo models using HbAS trait blood samples, which do not fully replicate the complex in vivo microenvironment of homozygous HbSS sickle cell disease patients. Second, the phytochemical characterization remains qualitative and lacks quantitative high-performance liquid chromatography (HPLC) or mass spectrometry (LC-MS) profiles to pinpoint and isolate the specific bioactive principles. Finally, further in vivo toxicity and pharmacokinetic studies are mandatory to evaluate the structural integrity and metabolic safety of these extracts before assessing any potential therapeutic development.

Conclusion:-

This study provided a rigorous chemometric and comparative pharmacological validation for the traditional use of *Alstonia boonei* (ABW) and *Enantia chlorantha* (ECO) stem barks harvested in Gabon (Franceville and Libreville) for the management of sickle cell disease. Quantitative evaluations exposed a major polarization in specialized biosynthetic pathways: *A. boonei* was characterized by a superior total phenolic density and proanthocyanidin load, whereas *E. chlorantha* exhibited a massive upregulation of core flavonoid frameworks (341.10 ± 6.77 mg QE/g).
Pharmacologically, both aqueous extracts demonstrated exceptional, dose-dependent anti-inflammatory efficiencies, significantly outperforming diclofenac sodium in preventing bovine serum albumin thermal denaturation and matching its erythrocyte membrane stabilization capacity. Furthermore, they exhibited a strong ability to prolong whole-blood clotting times (up to 45.32 min for ECO), offering key therapeutic avenues to mitigate thromboembolic complications *in vivo*.

Under controlled chemical hypoxia ($Na_2S_2O_5$), both Gabonese plant matrices induced an outstanding *ex vivo* morphological reversion, achieving a stable phenotypic normalization plateau of ~75% and statistically outclassing the clinical reference drug hydroxyurea, whose efficacy collapsed in this acellular setup. This anti-sickling mechanism **may be driven** by the passive transmembrane diffusion of polar anthocyanins, water-soluble phenolic acids, and **literature-reported** indole (echitamine) or isoquinoline (palmatine) alkaloids, **potentially** blocking polymer nucleation through direct ligand-protein interactions. However, the narrow therapeutic window of *A. boonei* (hepatotoxic and nephrotoxic liabilities at doses $\geq$ 400 mg/kg) highlights the critical need for strict dosage standardization. Taken together, these findings confirm that the multi-target chemical synergy of these crude barks represents a highly promising foundation for developing affordable, high-quality phytomedicines to manage sickle cell disease in sub-Saharan Africa.

References:-

1.Thomson AM, McHugh TA, Oron AP, Teply C, Lonberg N, Vilchis Tella V, et al. Global, regional, and national prevalence and mortality burden of sickle cell disease, 2000–2021: a systematic analysis from the Global Burden of Disease Study 2021. Lancet Haematol. août 2023;10(8):e585-99. doi:10.1016/S2352-3026(23)00118-7
2.Mburu J, Odame I. Sickle cell disease: Reducing the global disease burden. Int J Lab Hematol. mai 2019;41(S1):82-8. doi:10.1111/ijlh.13023
3.Delicat-Loembet LM, Mabiala AN, Bisvigou U, Avoune E, Bongo S, N'Tchoreret A, et al. Diagnosis of sickle cell disease in Gabon using sickle SCAN®: a point-of-care blood test. Int J Transl Med Res Public Health. 2022;6(2):1-9.
4.RGPL. Résultats globaux du Recensement Général de la Population et des Logements de 2013 DU Gabon (RGPL2013). 2013;259.
5.Kato GJ, Piel FB, Reid CD. Gaston MH, Ohene-Frempong K, Krishnamurti L, Smith WR, Panepinto JA, Weatherall DJ, Costa FF, Vichinsky EP. Sick Cell Dis Nat Rev Primer. 2018;4:18010.
6.Kavanagh PL, Fasipe TA, Wun T. Sickle cell disease: a review. Jama. 2022;328(1):57-68.
7.Araújo ADS, Silva Pinto AC, Lobo CLDC, Figueiredo MS, Menosi Gualandro SF, Olalla Saad ST, et al. Novel Insights into the Pathophysiology and Treatment of Sickle Cell Disease. Hemoglobin. 4 mars 2023;47(2):71-9. doi:10.1080/03630269.2023.2211771

8.Colombatti R, Jastaniah W, Makani J, Andemariam B. Sickle cell disease. The Lancet. mars 2026;407(10533):1095-111. doi:10.1016/S0140-6736(25)02278-0
9.Ngbolua KN, Rafatro H, Rakotoarimanana H, Ratsimamanga US, Mudogo V, Mpiana PT, et al. Pharmacological screening of some traditionally-used antimalarial plants from the Democratic Republic of Congo compared to their ecological taxonomic equivalence in Madagascar. Int J Biol Chem Sci. 2011;5(5):1797-804.
10.Mpiana PT, Tshibangu STD. Les alicaments et la drépanocytose: une mini-revue. Comptes Rendus Chim. 2016;19(7):884-9.
11.Ngbolua KTN, Tshilanda DD, Falanga CM, Ashande MC, Tshibangu DST, Iteku JB, et al. Anti-Sickle Cell Anemia and Bacterial Inhibitory Effects of Uvariodendron molundense (Diels) R.E.Fr. (Annonaceae) from Ubangi River Basin, DR Congo. J Biosci Med. 10 mars 2017;5(3):3. doi:10.4236/jbm.2017.53008
12.Ejele AE, Akpan IO, Ogukwe CE, Onyeocha VO, Ukiwe LN. Bioassay-guided isolation and partial characterization of an antisickling compound from Enantia chlorantha. Int J Biosci Biochem Bioinforma. 2012;2(7):149-54.
13.Walker R, Sillans R. Les plantes utiles du Gabon. Sépia. 1961:614.
14.Tcheghebe OT, Tatong FN, Seukep AJ. Traditional uses, phytochemical and pharmacological profiles, and toxicity of Enantia chlorantha (Oliver): An overview. Edorium J Med. 2016;3:12-8.
15.Davares AKL, Arsene MMJ, Viktorovna PI, Shommya D. Enantia chlorantha and its multiple therapeutic virtues: a mini review. J Pharm Res Int. 2021;33:254-9.
16.Evbuomwan IO, Adeyemi OS, Oluba OM. Aqueous extract of Enantia chlorantha Oliv. demonstrates antimalarial activity and improves redox imbalance and biochemical alterations in mice. BMC Complement Med Ther. 24 févr 2025;25(1):73. doi:10.1186/s12906-025-04745-w
17.Egunyomi A, Moody JO, Eletu OM. Antisickling activities of two ethnomedicinal plant recipes used for the management of sickle cell anaemia in Ibadan, Nigeria. Afr J Biotechnol. 2009;8(1):020-5.
18.Adotey JPK, Adukpo GE, Opoku Boahen Y, Armah FA. A Review of the Ethnobotany and Pharmacological Importance of *Alstonia boonei* De Wild (Apocynaceae). ISRN Pharmacol. 30 juill 2012;2012:1-9. doi:10.5402/2012/587160
19.Ambomo NF, Gounoue RK, Donfack JH, Ngueguim FT, Bidja AC, Dzeufiet PDD, et al. Aqueous extract of Alstonia boonei De Wild (Apocynaceae) alleviates bone metabolism disorders induced by oxidised palm oil and sucrose supplementation in rats. J Phytopharm. 2024;13(3):197-207.
20.Adesina AF, Apata JT, Babalola OO, Otuechere CA, Adekola MB, Ogunleye GS, et al. Hepatoprotective activity of Alstonia boonei (De Wild) stem bark in isoniazid-induced Wistar rats: Antioxidant, anti-inflammatory and in silico evaluations. Pharmacol Res-Mod Chin Med. 2025;14:100558.
21.Ileke KD, Adesina JM, Abidemi-Iromini AO, Abdulsalam MS. Entomocide effect of Alstonia boonei De wild on reproductive performance of Dermestes maculatus (Coleoptera: Dermestidae) infestation on smoked catfish Claria gariepinus (Pisces: Clariidea). Int J Trop Insect Sci. juin 2021;41(2):1293-304. doi:10.1007/s42690-020-00321-6
22.Olanlokun OJ, Olorunsogo OO. Toxicology of solvent extract and fractions of Alstonia boonei (DC.) Wild stem bark in Rats. J Herbmed Pharmacol. 2018;7(3):129-35.
23.Harborne AJ. Phytochemical methods a guide to modern techniques of plant analysis. 3rd ed. London: Chapman & Hall; 1998.
24.Sofowora A. Recent trends in research into African medicinal plants. J Ethnopharmacol. 1993;38(2-3):197-208.
25.Singleton VL, Orthofer R, Lamuela-Raventós RM. [14] Analysis of total phenols and other oxidation substrates and antioxidants by means of folin-ciocalteu reagent. Methods in enzymology. 1999;299:152-178.
26.Quettier-Deleu C, Gressier B, Vasseur J, Dine T, Brunet C, Luyckx M, et al. Phenolic compounds and antioxidant activities of buckwheat (Fagopyrum esculentum Moench) hulls and flour. J Ethnopharmacol. 2000;72(1-2):35-42.
27.Communauté européenne. The reference method of European community was used to measure total amount of Tannins. 1994.
28.Prigent S. Interactions of phenolic compounds with globular proteins and their effects on food-related functional properties. Wageningen University and Research; 2005. 1-132 p.
29.Ngoua-Meye-Misso RL, Sima-Obiang C, Ndong JDLC, Ondo JP, Abessolo FO, Obame-Engonga LC. Phytochemical screening, antioxidant, anti-inflammatory and antiangiogenic activities of Lophira procera A. Chev.(Ochnaceae) medicinal plant from Gabon. Egypt J Basic Appl Sci. 2018;5(1):80-6.
30.Tepe B, Daferera D, Sokmen A, Sokmen M, Polissiou M. Antimicrobial and antioxidant activities of the essential oil and various extracts of Salvia tomentosa Miller (Lamiaceae). Food Chem. 2005;90(3):333-40.
31.Engonga O, Timoléon AB, Joseph-Privat O, Ludovic M, Roger NAG, Fatouma AL, et al. Total phenolic composition, antibacterial and antioxidant activities of Fagara heitzii Aubr. & Pellegr. medicinal plant of Gabon. Vedic Res Int Phytomedicine. 2 nov 2013;1(3):85. doi:10.14259/pm.v1i3.50

32.Scherer R, Godoy HT. Antioxidant activity index (AAI) by the 2, 2-diphenyl-1-picrylhydrazyl method. Food Chem. 2009;112(3):654-8.
33.Kubola J, Siriamornpun S. Phenolic contents and antioxidant activities of bitter gourd (Momordica charantia L.) leaf, stem and fruit fraction extracts in vitro. Food Chem. 2008;110(4):881-90.
34.Pavithra R, Khan MR, Khan MS. In vitro evaluation of phytochemical, antioxidant, anti-inflammatory and anticancer properties of Suaeda maritima. Discov Appl Sci. 3 juin 2025;7(6):594. doi:10.1007/s42452-025-06912-7
35.Williams L, Connar AO, Latore L, Dennis O, Ringer S, Whittaker J, et al. The in vitro anti-denaturation effect induced by natural products and non-steroidal compounds on heat-treated bovine serum albumin. West Indian Med J. 2008:327-31.
36.Emmel VE. A red cell study of the erythrocytes in a case of severe anemia with elongated and sickle-shaped red blood corpuscles. Arch Int Med. 1933;7:769-89.
37.Lee RI, White PD. A clinical study of the coagulation time of blood. Am J Med Sci 1827-1924. 1913;145(4):495.
38.Ramdé-Tiendrébéogo A, Tibiri A, Ouedraogo M, Ouédraogo S. Study of Antisickling and Vasorelaxant Activities and Acute Toxicity Assessınent of Crude Extracts of Leaves of Ficus syconnorus L.(Moraceae). Pak J Biol Sci. 2014;17(6):829-35.
39.Madiélé AB, Quio Zhao JM, Thiéry V, Agnaniet H, Brunet C, Graber M, et al. Caractérisations analytiques des extraits colorants des plantes tinctoriales d'Afrique Centrale. Leban Sci J. 2015;16(1):33-33.
40.Alsultan AI, Seif MA, Amin TT, Naboli M, Alsuliman AM. Relationship between oxidative stress, ferritin and insulin resistance in sickle cell disease. Eur Rev Med Pharmacol Sci. 2010;14(6):527-38.
41.Phelan M, Perrine SP, Brauer M, Faller DV. Sickle erythrocytes, after sickling, regulate the expression of the endothelin-1 gene and protein in human endothelial cells in culture. J Clin Invest. 1995;96(2):1145-51.
42.Kambale JK, Ngolua KN, Mpiana PT, Mudogo V, Tshibangu DST, Wumba DMR, et al. Evaluation in vitro de l'activité antifalcémiante et effet antioxydant des extraits d'Uapaca heudelotii Baill.(Euphorbiaceae). Int J Biol Chem Sci. 2013;7(2):523-34.
43.Mpiana PT, Dianzenza EN, Ngbolua KN, Tshibangu DST, Mbala BM, Mhigo SO, et al. Antisickling properties, thermal and photochemical degradations of anthocyanin extracts from Annona senegalensis (Annonaceae). Int J Biol Chem Sci. 2012;6(5):2241-51.
44.Sandoval-Castro CA, Torres-Acosta JFJ, Hoste H, Salem AZM, Chan-Pérez JI. Using plant bioactive materials to control gastrointestinal tract helminths in livestock. Anim Feed Sci Technol. 2012;176(1-4):192-201.
45.Zarghamian P, Klermund J, Cathomen T. Clinical genome editing to treat sickle cell disease—a brief update. Front Med. 2023;9:1065377.
46.Ramde-Tiendrebeogo A, Koala M, Ouedraogo G, Ouedraogo N, Kini FB, Chalard P, et al. Utilisation des feuilles de Ficus sycomorus L.(Moraceae) dans la prévention de l'hypercoagulation chez les drépanocytaires: identification de composés phénoliques potentiellement anticoagulant et antiagrégant plaquettaire. Int J Biol Chem Sci. 2019;13(2):824-35.
47.Seakins M, Gibbs WN, Milner PF, Bertles JF. Erythrocyte Hb-S concentration An important factor in the low oxygen affinity of blood in sickle cell anemia. J Clin Invest. 1973;52(2):422-32.
48.Lokonon JE, Tchogou P, Agbogba F, Abissi G, Medoatinsa E, Koudoro Y, et al. Anti-sickling activity of Daniellia oliveri (Rolfe) Hutch. & Dalziel. bark aqueous extracts in the management of sickle cell disease in Benin. J Appl Biosci. 2021;168(1):17446-55.
49.Mellouli F, Bejaoui M. The use of hydroxyurea in severe forms of sickle cell disease: Study of 47 Tunisian paediatric cases. Arch Pediatr Organe Off Soc Francaise Pediatr. 2007;15(1):24-8.
50.Prigent SVE, Voragen AGJ, Van Koningsveld GA, Baron A, Renard CM, Gruppen H. Interactions between globular proteins and procyanidins of different degrees of polymerization. J Dairy Sci. 2009;92(12):5843-53.